



Reconstructing long-term gully dynamics in Mediterranean agricultural areas

Antonio Hayas¹, Tom Vanwalleghem¹, Ana Laguna², Adolfo Peña³, and Juan V. Giráldez^{1,4}

¹University of Cordoba, Dept. of Agronomy, da Vinci Bldg., Cra Madrid km 396. 14071 Córdoba, Spain

²University of Cordoba, Dept. of Applied Physics, Einstein Bldg.

³University of Cordoba, Dept. of Rural Engineering, da Vinci Bldg.

⁴Institute for Sustainable Agriculture, CSIC, Dept. of Agronomy, Alameda del Obispo, 14080 Córdoba, Spain

Correspondence to: A. Hayas, z22haloa@uco.es

Abstract. Gully erosion is an important erosive process, especially in Mediterranean basins. However, the long-term dynamics of gully networks and the variation of sediment production in gullies is not well known. Available studies are often done over a few years only, while many gully networks form, grow, and change in response to environmental and land use or management changes over a long period. In order to clarify the effect of these changes, it is important to analyze the evolution of the gully network with a high temporal resolution. This study aims at analyzing gully morphodynamics over a long time scale (1956-2013) in a large Mediterranean area in order to quantify gully erosion processes and its contribution to overall sediment dynamics.

A gully network of 20 km² located in SW Spain, has been analyzed using a sequence of 10 aerial photographs in the period 1956-2013. The extension of the gully network both increased and decreased in the study period. Gully drainage density varied between 1.93 km km⁻² in 1956, with a minimum of 1.37 km km⁻² in 1980 and a maximum of 5.40 km km⁻² in 2013. The main controlling factor of gully activity appeared to be rainfall, while land use changes were found to have only an indirect effect. A new Monte Carlo-based approach was proposed to reconstruct gully erosion rates from orthophotos. Gully erosion rates were found to be relatively stable between 1956-2009, with a mean value of 11.2 ton ha⁻¹yr⁻¹, while in the period 2009-2011, characterized by extreme winter rainfalls, this value increased significantly, to 591 ton ha⁻¹yr⁻¹. These results show that gully erosion rates are highly variable and that a simple interpolation between the start and end date would highly underestimate gully contribution during certain years, such as for example between 2009-2011. This illustrates the importance of the applied methodology using a high temporal resolution of orthophotos.

1 Introduction

Understanding gully erosion dynamics under changing land use and climate conditions is essential for soil and water conservation especially in Mediterranean areas. Erosion is one of the most significant threats to soils and sustainable agriculture worldwide (Amundson *et al.*, 2015). To satisfy long-term food production and food security, soil erosion rates must be drasti-



cally reduced to the level of soil formation rates. Additionally the sediment dispersion induces environmental pollution, with severe downstream problems to infrastructure. Soil erosion is a major factor in the anthropogenic perturbation of the global carbon cycle (Regnier *et al.*, 2013). Given the importance of soil erosion, much research effort has gone into characterizing and modelling erosion rates in order to identify key problem areas and propose management solutions. Recently, a European-wide effort was done to improve the quantification of water erosion either with RUSLE (Panagos *et al.*, 2015), or with similar models (Quinton *et al.*, 2010; Van Oost *et al.*, 2007). Nevertheless, such models represent a minor part of the water erosion processes, not considering the contribution of gullies. Poesen *et al.* (2002), concluded that gully erosion could be the source of up to 83% of sediment yield of Mediterranean areas. Recent efforts to measure gullies in detail confirm these numbers. For instance Castillo (2012) estimated the range of gully erosion rate in a set of cultivated catchments in Cordoba in 37 to 250 ton $\text{ha}^{-1}\text{yr}^{-1}$.

Most erosion models for gully erosion focus on modelling headcut growth. Examples are REGEM, its adaptation TIEGEM, both used in the model Annualized AGricultural Non-Point Source (AnnAGNPS; Gordon *et al.*, 2007; Taguas *et al.*, 2012), CHILD (Flores-Cervantes *et al.*, 2006; Campo-Bescós *et al.*, 2013) or the headcut growth model by Rengers and Tucker (2014). Kirkby and Bracken (2009) presented an areal gully growth model that showed how the ratio of channel versus sidewall processes is a key determinant in its evolution. In contrast, Dabney *et al.* (2015) model gully erosion rates by shear by inserting a new Ephemeral Gully Erosion Estimator, (EphGEE), included in a new version of RUSLE2, in a small agricultural watershed in Iowa. More mathematically based models look for general laws controlling areal gully growth and ramification (*e.g.* Devauchelle *et al.* 2012). More research will be needed in order to develop full three-dimensional models, capable of accurately predicting gully erosion volumes. In general however, there is an important lack in suitable field data for understanding and modelling long-term gully evolution. Due to the recent nature of most studies on gully erosion, their temporal coverage is limited to a few years at best. More recent studies usually focus on one specific moment in time, where the gully system is visited and measured once or during a couple of years. This implies that any dynamic behaviour of the gully system cannot be described adequately and that it is difficult to single out the controlling processes. Growth of gully systems in the Belgian loess belt was shown by Vanwalleghem *et al.* (2005) to be a highly non-linear process, with a rapid initial growth followed by a stabilization phase. Under different climates, especially under a Mediterranean climate, where rainfall is less uniform and much more concentrated, such non-linear gully dynamics can be expected to be accentuated. It may therefore turn out that a single measurement of a gully volume that has been growing for several decades, will not offer a good estimate of yearly growth rates. Gully growth can be expected to be much higher during specific years compared to the long-term mean. Any model efforts will therefore need experimental data collected with a high temporal resolution.

Over such longer time scales, exceeding several decades, little experimental data is available. Over the very long time scale of up to several centuries, different studies indicate that gully erosion is not a new process. In Northern and Central Europe, gullies have been dated between Early Bronze Age and Late Medieval times (Vanwalleghem *et al.*, 2006). In the Western Mediterranean, with a long history of land use, such historical studies are rare however (Dotterweich, 2013). Over the medium



term, of several decades, available studies also point to an important dynamic of ephemeral gullies, with erosion phases and phases of infilling. These can be due to normal tillage operations for small, ephemeral gullies; deliberately by farmers in case of larger gullies; or during phases of land use change where farmers erase such topographic features by tillage, as supported by field evidence. Gordon *et al.* (2008) showed by simulations using the REGEM model that such cycles of erosion and infilling could produce up to double the amount of sediment as when gullies were left to erode naturally. Each infilling phase prepares sediment for the next important storm event. Field data for this time scale are rare and generally comes from the analysis of historical air photos. Frankl *et al.* (2013) quantified the evolution of a permanent gully network in Ethiopia using long-term historical air photos over the period 1963–2010 for an area of 123 km². After an initial stability phase, they identified a peak erosion period in 1994, after which the system stabilized again. These results stress the importance of intensive temporal observations. Saxton *et al.* (2012) analysed multitemporal aerial photographs between 1951 and 2006 to derived historical gully erosion rates in terms of superficial growth per year in three catchments in south-east Queensland in Australia and, associated the gully initiation to post-European settlement land use practice and above average rainfall and runoff. Other methods have been tested, such as using local farmer knowledge on gully morphology (Nyssen *et al.*, 2006; Tebebu *et al.*, 2010) or using multi-temporal oblique photography of gully cross sections (Frankl *et al.*, 2011), but the uncertainty on the results is generally too high to allow a quantitative analysis of controlling climate or land use factors.

The objective of this study is then to quantify the erosion and infilling dynamics of a gully network in a typical agricultural area of SW Spain, from historical air photos between 1956 and 2013. A new method is presented that not only allows to determine the evolution of gully length, but also, by using Monte Carlo analysis to generate gully width and depth, to calculate the volume of gully erosion and infilling and to constrain the uncertainty. Moreover, the controls in terms of land use and rainfall variability are analysed and the importance of these results for the regional sediment budget is assessed.

2 Materials and methods

2.1 Study site

The study area is located between 37.74 and 37.81° N, 4.36 and 4.43° W, in the West Campiña of the Guadalquivir basin in the SW Spain (Fig. 1) and comprises an area of 20.6 km². The studied gully network drains towards a series of small ephemeral rivers (Arroyo de Garuñana, Arroyo del Cuadrado, Arroyo del Pozo Muerto, Arroyo de las Monjas, and Arroyo del Barranco), which all drain to the Guadajoz, a tributary of the Guadalquivir river. Although the limits between rills, gullies and larger ephemeral river channels are subject to discussion in the scientific community, this ephemeral river network was not included in the analysis, as it is indicated on the topographical maps and assumed stable. The observed gullies can be considered mostly permanent, although some ephemeral ones are also included as long as they have a width equal to or higher than the resolution of the orthophotos that were used, ranging between 0.5 and 1.0 m (Table 1).



Gentle hills prevail in the study area except from the south and the centre east where steeper ones exist (up to 32%). Altitudes range from 233 to 558 m high and mean slopes are 13%. The soils in the area are dominated by Vertisols, formed mainly in marls and calcareous sandstones deposited during the Miopliocene.

Currently the dominating land uses are olive orchards and herbaceous crops covering almost the whole area, except some 5% of the surface area occupied by grassland. Mean annual precipitation varies between 500 and 600 mm (Córdoba Airport station and Baena RIA station). The distribution of the precipitation shows a marked dry season between June and September while the main wet period occurs from October to May.

2.2 Rainfall characterization

Characterization of the rainfall regime was performed from daily rainfall collected in the period 1956-2013 at Castro del Río meteorological station (37.69° N, 4.47° W), belonging to the Spanish National Meteorological Agency (AEMET). Isolated data gaps between 1970 and 1971 were completed from the data recorded at Cañete de las Torres meteorological station (37.83° N, 4.36° W, Phytosanitary Warnings Network of Andalusia, RAIF) and Córdoba Airport meteorological station (37.84° N 4.84° W, AEMET). Anomalies in annual rainfall were evaluated by means of normalization, through average and standard deviation of annual rainfall for a 57 years period (1956-2013), following Martínez-Casasnovas *et al.* (2003). Values falling outside the interval R_{mean} (average rainfall) \pm sd (standard deviation), which correspond to the normalized values >1 and <-1 , were considered anomalies.

The frequency distribution of daily rainfall above a threshold value of 13 mm was analysed, considering this as the minimum rainfall that produces erosive effects as proposed by Wischmeier and Smith (1978) and Renard *et al.* (1997). In addition, frequency distribution of records above the average daily rainfall event plus the standard deviation were also analysed, assuming that these events represent the extreme rainfall events within the study period.

2.3 Photointerpretation process

Analysis of gully evolution and land use change was conducted by photointerpretation based on a dataset of aerial orthophotos of different years from 1956 to 2013. Performance characteristics of the orthophotos dataset are summarized in Table 1. The working scale in the photointerpretation processes was established to 1:5000 for the whole dataset.

2.3.1 Land use

Land use in the study area for 2001, 2005, 2009, 2011, and 2013 was derived from the respective orthophotos while for the rest of the years (1956, 1980, 1984, 1999, 2003, and 2007) existing Maps of the Land Use and Vegetation Cover of Andalusia (Red de Información Ambiental de Andalucía, REDIAM) were used. Different land uses present in the area were simplified to three classes as shown in Table 2.



2.3.2 Gully network length

Gully length was obtained by digitizing the extension of the gully network for each available year, distinguishing between newly incised and infilling stretches. Gully network was decomposed in m_y segments, where subscript y indicates the year. Each segment comprises the length between consecutive junctions (Fig. 2). Due to changes in the drainage network during the study period, the number of segments ranged between 108 in 1980 and 940 in 2013. The total length of the drainage network for a given year, L_y , was calculated as the sum of the lengths of individual segments, $l_{y,i}$

$$L_y = \sum_{i=1}^{m_y} l_{y,i} \quad (1)$$

with m_y equal to the total number of individual segments of the gully network for each digitalized year.

2.3.3 Gully network width

In order to measure gully width in a representative way, 35 stretches were selected from the earliest digitalized gully network of 1956, covering a wide range of widths. Gully width was measured at the same locations on later orthophotos, allowing the evaluation of the widening process during the complete study period.

2.4 Field campaign

During 2013 and 2014 several field campaigns were conducted to measure current gully widths and depths with measuring tape and a clinometer (Suunto PM-5/360 PC). Gully top width and depth were measured at 27 representative sections distributed randomly over the gullies catchments. These representative sections covered the entire range of width and depth variability, including different landscape positions, from upstream close to the divide to the junction with the stream network, and both in gullies on herbaceous crops and under olive orchards gullies.

2.5 Monte Carlo-based simulations

Although gully length for the different years between 1956 and 2013 could be determined directly from observations using the available air photographs, determination of the gully volume was not straightforward. As we used freely available orthophotos, it was only possible to measure the size of the gullies in two dimensions and no measure of depth was readily available. Also observations of gully width for each year were limited to the representative sections measured on the orthophotos of that particular year and therefore included a term of uncertainty as the real population mean remained unknown. Estimation of overall gully network volume for each year, \bar{V}_y , was therefore tackled by conducting a Monte Carlo simulation in which a volume and an associated uncertainty were calculated for every single gully segment, $l_{y,i}$, described in paragraph 2.3.2 (Fig. 2).



For each year, y , a set of $n = 1000$ estimated cross area sections, $S_{y,i} = \{s_{y,i,j}, j = 1, \dots, n\}$ for every single segment, $l_{y,i}$, were generated as show in Figure 3, which required the generation of sets of width and depth values for each year. Each generated section is calculated as

$$s_{y,i,j} = kw_{y,i,j}d_{y,i,j} \quad (2)$$

5 where k is a shape factor, and $w_{y,i,j}$, and $d_{y,i,j}$, the simulated gully width and depth respectively. Field observations suggested that a triangular section is a reasonable approximation of most gully sections, so a shape factor $k = 0.5$ was adopted in order to compute the simulated sections.

To generate a representative measure of gully width, first of all, the gully width distribution measured for each year by photointerpretation at the representative sections was fitted to different probability distribution functions (normal or Gaussian, gamma,
 10 lognormal, exponential and Weibull) using the maximum likelihood method. Next, goodness of fit was evaluated for these different distributions by means of the Kolmogorov-Smirnov statistics. Finally, the best overall fitting theoretical probability distribution was selected to obtain the necessary parameters (μ_y, σ_y) to generate n random simulations of representative gully widths for any particular year.

The estimation of gully depth for each year was based on the field data gathered in 2013-14. In order to estimate depth for
 15 previous years, firstly a width-depth relationship was estimated by linear regression analysis from the collected field data. Such a relationship could only be established for the present-day situation. Uncertainty on this linear width-depth relation was then taken into account by computing the estimated intercept, slope and their respective standard deviations (a, b, s_a, s_b) . Assuming a normal distribution, a set of one thousand slope and intercept pairs were simulated. Depths for unique segments $(D_{y,i})$ were then derivate from simulated widths and slope-intercept pairs.

20 Finally, a set of n simulated volumes $V_{y,i} = \{v_{y,i,j}, j = 1, \dots, n\}$ was calculated for each year and segment multiplying individual measured lengths by the simulated sections (Fig. 3)

$$v_{y,i,j} = s_{y,i,j}l_{y,i} \quad (3)$$

A set of n different simulated volumes of the complete gully network for a particular year V_y was eventually calculated as the sum of volumes of single segments $v_{y,i,j}$

$$25 \quad V_y = \{v_{y,i,j}, j = 1, \dots, n\} \quad (4)$$

and

$$v_{y,j} = \sum_{i=1}^{m_y} v_{y,i,j} \quad (5)$$

Finally average volume of the total gully network for a given year, \bar{V}_y , was computed as

$$\bar{V}_y = \frac{1}{n} \sum_{j=1}^n v_{y,j} \quad (6)$$



Erosion rates were then obtained from the different between pairs of simulated volumes in consecutive dates divided by the duration of the period.

3 Results

3.1 Rainfall characteristics during the study period

5 The annual rainfall depths in the analysed period ranged between 180 mm in the hydrological years 2004/2005 and 973 mm in 2009/2010, with an average value of 546 mm (Table 3). Figure 4 shows standardized annual rainfall between 1956 and 2013 and the anomalies of annual rainfall. Annual rainfalls greater than the 0.75 percentile (656 mm) were registered in 15 occasions of which 10 surpassed the average annual rainfall plus the standard deviation (748 mm). Among the lapses between aerial orthophotos dataset, the period 1984-1999 and 2009-2011 concentrated the major number of positive extreme annual rainfalls.

10 In 1984-1999 eight out of fifteen records were greater than the 0.75 percentile, and 6 of them were considered anomalies since they were greater than the average annual rainfall plus the standard deviation. In the period 2009-2011, both years recorded annual rainfall amounts higher than the standard deviation and can thus be considered an anomalous extreme rainy period. Figure 5 shows the distribution of the 3698 daily rainfall events recorded during the study period. Daily rainfall events (R_{24}) higher than 13 mm accounted for 21.7% of the total registered. Among the different periods the highest proportion of $R_{24} > 13$

15 mm were recorded in 2009-2011 (27.5 events per year, Table 3) whereas the average proportion was 13.9 R_{24} events > 13 mm per year. Rain depths higher than the average value (8.4 mm) plus the standard deviation (10.8 mm) were considered extraordinary events, which were concentrated in major proportion in the periods 1984-1999 (10.5 records per year) and 2009-2011 (13 records per year) (Table 3). Maximum daily rainfalls were registered in the hydrological years 1997/1998 (140 mm) and 2007/2008 (126 mm), with an average value of 48.68 mm for the entire period.

20 3.2 Land use change

Land use experienced a progressive conversion from herbaceous crops to olive orchards as shown in Figure 6. In the study period, olive orchards grew from 13% to 63% of occupation of the land use in the study area. At the same time herbaceous crops decreased from 85% to 35% of the occupied land. The main land use change occurred between 1984 and 1999, when the olive orchards passed from occupying 25% to 48% of the total area. The highest rates of change however were observed in the

25 period 2005-2007 with more than 4% rate of annual land use change from herbaceous crop to olive orchards.

3.3 Gully network length dynamics

Figure 7 shows the evolution of the gully network derived by photo-interpretation between 1956 and 2013. Drainage density is included there. From 1956 to 2013 the gully network increased not only in length but in number of branches as well. Further



analysis on the length and area ratio showed that the drainage density has grown from 17.2 m ha^{-1} to 53.3 m ha^{-1} . In most of the analyzed period variations on drainage density occurs are small. However, there are two significant periods where the increase is very high and that account for the main increases in the overall value. From 1984 to 1999 and 2009 to 2011 there was an increment of 14.6 m ha^{-1} and 23.6 m ha^{-1} respectively, which account for 84% of the total drainage density growth. When comparing these gully length dynamics to controlling factors of land use and rainfall, it can be seen in table 3 that these rapid growth could be related to extreme rainfall events that occurred in 1997 and anomalous rainy periods in 2009-2011. In contrast, in some periods as for instance in 1956-1980, 1999-2001, 2001-2005 and 2007-2009 the gully network experimented several decreases in the drainage density, although in no case this decrease was more than 4 m ha^{-1} , and can therefore be considered modest. These decreases can be directly related to farming operations where farmers fill in the upstream gully stretches that are limited in depth and can be considered ephemeral gullies.

Figure 8 shows the frequency distribution of headcut growth and infilling of individual gullies for the different periods between 1956-2013. Some of the observation periods show a balance between infilling and growing reaches, which leads to a very minor overall change of the total gully network length. During a few distinct intervals however, 1984-1999 and 2009-2011, this balance shifts drastically and results in a fast increase of the gully network's total length, as can be seen in Figure 9. This can be in part explained because in these two periods infillings are almost negligible (Fig. 8 and Fig. 9). However, in Figure 9 growth of the gully at the end of those periods (1999 and 2011) is much higher (31 km and 49 km) than those from the other end periods (13 km as the highest value), which clearly shows that gully growth is the dominant process controlling gully dynamics in those periods.

Figure 9 shows how the total length of the gully network tripled from 35.4 km in 1956 to 109.8 km in 2013 (Fig 9). Main enlargements periods were registered in 1980-1984 (10.6 km), 1984-1999 (29.9 km) and 2009-2011 (48.8 km). In contrast, during some other periods, as for instance in 1956-1980, 1999-2001, 2001-2005 and 2007-2009, the balance between infilling and growing stretches resulted in a net reduction of the total gully network length. Infilling gully stretches identified during photointerpretation, may be classified in two different types: those made while regular tilling operations at the end of the summer, usually in the order of several tens of meters and those resulting from land levelling during phases of land use change, which may reach some hundreds of meters.

Extraordinary annual rainfalls as well as individual extreme precipitation events seem to be the main factors that can be linked to gully retreat (Table 3). Land use does not seem to control these observed peaks in gully length increase directly. However, land use change could have contributed to the rainfall extremes inducing high peak discharges, because since 1956 a shift from cereal crops to olive orchards occurred in half of the study area, and which was especially intensive from 1984 forward. Young olive trees with limited root systems and small canopies leave an important bare soil surface and little protection to overland flow or gully headcut advance. However, further analysis should be done in order to confirm this hypothesis.



3.4 Gully network width dynamics

Top width at the representative cross sections, as derived from the orthophotos dataset, experienced a continued widening over time (Fig. 10). While at the beginning of the study period (1956), the maximum top width was close to 12.0 m, this value progressively increased over subsequent years, until reaching a maximum value of 59.0 m in 2013. Average value increased smoothly from 4.5 m wide in 1956 to 8.0 m in 2005, whereas the rate of increase for the period 2005–2013 clearly got steeper, resulting in final average width of 13.1 m in 2013. Although widening could be expected at every time step, average widths derived from the cross sections in 2007 (7.7 m) actually experienced a narrowing with respect to those measured in 2005 (8.0 m). Since this period (2005–2007) experimented the highest rate of land use change in the series, this reduction in cross section could be explained to the reopening of gullies that had previously been removed by land levelling during a land use shift to olive orchards.

Table 4 summarize p-values obtained by means of the Kolmogorov-Smirnov statistic, which was used to evaluate the suitability of different theoretical probability distributions for fitting the observed top widths. The lognormal distribution showed to be the most suitable for almost all the years, with highest p-value of 0.98, in 1980 and 1999 and lowest p-value of 0.64 for 2011, although it was still the best fit from all tested distributions. These fitted probability distributions were then used to simulate 1000 random widths for each year and single segment composing the gully network.

3.5 Width and Depth relationship

In order to compute the volume of the gully network, depths at the different stretches were derived from the Monte Carlo simulated widths using a width-depth relation derived from field work, shown in Figure 11. A coefficient of determination $R^2 = 0.83$ was obtained from a logarithm-based fitting, with slope, intercept and their standard deviation respectively 1.73 ± 0.16 and 0.55 ± 0.32 . Normal deviates based on those coefficients were used to generate 1000 width and depth pairs.

3.6 Gully volume dynamics

Figure 12 presents the final volume evolution, as calculated by means of the Monte Carlo simulation. Gully stretches with a unique, observed length were multiplied by the generated width and depth pairs, resulting in 1000 simulated gully network volumes for each stretch and for each period. Average volume in addition to minimum and maximum volume were then derived from the set of simulations, showing the growth of the gully in terms of mean eroded volume as well as a measure of uncertainty, by means of the 5-95% confidence interval of these inferences, shown in grey. Gully network volume grows from 0.18 hm^3 in 1956 to 3.24 hm^3 in 2013. These results show how the total gully volume has increased by 17 times its original value. Main periods of rapid volume growth occurred at the end of the study period, between 2009 and 2013, when the gully volume increased from 0.82 hm^3 until its final value of 3.24 hm^3 . Moreover, the period 2009–2011 alone accounts for nearly 52% of the observed growth. Infilling phases were also reflected in the volume evolution curve shown in Figure 12, as for



instance at the end of the period 1956-1980 when gully volume decreased until it reached its minimum value (0.15 hm^3), and in 2007 which shows a 0.015 hm^3 decrease from the average volume in 2005 (0.81 hm^3).

3.7 Gully erosion rate dynamics

Dynamics of gully erosion rate are shown in Figure 13. Maximum erosion rate was reached in the period 2009-2011 when 591 $\text{ton ha}^{-1}\text{yr}^{-1}$ were lost according to the simulation process. Minimum erosion rate ($-5.21 \text{ ton ha}^{-1}\text{yr}^{-1}$) was registered in the period 2005-2007. Negative values here reflect the decrease of the gully network volume, and therefore should not be considered an erosion rate but an infilling rate. Average erosion rate for the whole study period was $39.7 \text{ ton ha}^{-1}\text{yr}^{-1}$.

4 Discussion

The average gully erosion rate of $39.7 \text{ ton ha}^{-1}\text{yr}^{-1}$ obtained in this study, by means of photo-interpretation techniques combined with stochastic methods, are of the same order of magnitude with those found in literature in Mediterranean basins. Oostwoud Wijdenes *et al.* (2000) reported erosion rates of $1.2 \text{ ton ha}^{-1}\text{yr}^{-1}$ in bank gullies developed into highly erodible sedimentary deposits in the southeast of Spain, derived by aerial photo analysis over a 38 year period. The highest gully erosion rate of $1,322 \text{ ton ha}^{-1}\text{yr}^{-1}$ was found by Martínez-Casasnovas *et al.* (2003) in large gullies in the NE Spain, from high resolution DEMs and GIS analysis in a 36 year period. Compared with other erosion processes, the gully erosion rates measured here almost double the average erosion rates for sheet and rill erosion reported for olive orchards in the Mediterranean ($23.2 \text{ ton ha}^{-1}\text{yr}^{-1}$) by Gómez *et al.* (2008). Olive orchards are one of the most important crops in the Mediterranean and are generally considered to be highly affected by sheet and rill erosion. This clearly stresses the importance of adequately considering gully erosion processes when modelling soil losses from water erosion.

Most importantly, the results show a wide variability in gully erosion rates, ranging between -5.21 and $591 \text{ ton ha}^{-1}\text{yr}^{-1}$. This includes periods dominated by infilling and rapid growth, underlining the importance of measuring erosion rates at the finest temporal resolution possible in order to overcome under- and/or overestimations in sediment production. Such variability is in part explained by the inherent irregularity of the local rainfall regime which appears to be the main controlling factor for gully erosion at this site. However, land use change has played an important role intensifying in some cases and masking in other cases the rates of gully erosion. For instance, in the initial period between 1956 and 1980, erosion rate shows a negative value. However, given the length of this period and since there are some particular years (*i.e.* 1961-1962) with extreme rainfalls it is likely that positive gully growth occurred during this period that was later masked by infilling. Moreover, the data presented here clearly show that in Mediterranean areas the gully growth dynamics are different than in temperate areas. A review of different studies on gully growth over time by Poesen *et al.* (2006) indicated a rapid initial growth, followed by a stable phase with slow growth for “mature” gullies. Data for this study was from the temperate loess belt or from lab experiments under constant discharge conditions. In our case, with a high variability in natural rainfall, even after several decades, intense growth



phases were observed. As stated before, these could mainly be attributed to an increase of the gully's cross sections, and less to a gully headcut retreat. Therefore, models such as CHILD or REGEM, which have been applied with success to gully modelling, but focus mainly on headcut activities, would probably not yield good results in this case.

From a wider geomorphological perspective, other phenomena such as lowering of the base level and incision of the river bed could be suggested as a cause of the progressive increase on the erosion rate. Nevertheless, there was no field evidence of this. In addition, the Guadalquivir river basin is a highly regulated river, with many dams, which could be expected to limit any such effects.

Gully erosion rates computed between the start and the end of the study period would incur in gross underestimation. Erosion rates between 1956 and 2009 are under the average ($39.7 \text{ ton ha}^{-1}\text{yr}^{-1}$), while the last period (2009-2013) accounted for around 52% of the gully volume growth, reaching a peak value of $590 \text{ ton ha}^{-1}\text{yr}^{-1}$ in the period 2009/2011. Nevertheless, these observations are in accordance with other studies in the Mediterranean. Gully erosion rates after some extreme rainfall events in the Mediterranean Basin has been reported to reach occasionally 207 ton ha^{-1} (Martínez-Casasnovas *et al.*, 2002). In a review of the western Mediterranean basin, González-Hidalgo *et al.* (2007) found that on average the three largest daily events per year accounted for more than 50% of the total sediment exported from the basin. The so-called time compression of Mediterranean climate with respect to soil erosion is therefore very high, as is demonstrated by the data from this study.

The Monte Carlo stochastic modelling performed also allow to identify that while gully length dynamics (Fig. 9) could explain some of the rapid increases in the volume and erosion rate computed, widening processes (Fig. 10) determine the shape of volume curve (Fig. 12) pointing out the importance of that parameter in the computed volume as opposite, in this particular case, as suggested by other authors who found for other areas and climates that the leading controlling parameter is gully length (Nachtergaele and Poesen, 1999). This observation will lead future field work and modelling efforts, which should not only consider gully headcut advance, but also on the mechanisms of gully sidewall collapse and erosion. Possibly a very important factor here, also in order to control the gully growth, is the effect that roots may have on stabilizing the gully walls (De Baets *et al.*, 2008).

The main advantage of the new method described here, is that by means of Monte Carlo simulation, an estimation of the uncertainty associate along with the measure of gully erosion volume is generated. This is especially relevant when suitable knowledge of erosion dynamics is required and management systems need to be evaluated or compared.

5 Conclusions

A new method was presented to evaluate gully growth over decadal time scales, combining airphotos interpretation with a stochastic approach through Monte Carlo modelling for the channel section parameters. This resulted to be a reliable procedure to determine gully network dynamics over time. Uncertainty ranges obtained in the simulation provide an unprecedented view on the gully network dynamics useful from a management perspective. Whereas highly variable, the observed erosion



rates were in accordance with previous studies in Mediterranean basins. The fluctuations in erosion rates were mainly attributed to the variability in rainfall regime variations, likely exacerbated by land use changes, although further research -using physical modelling of runoff, gully headcut retreat rates and sidewall dynamics- should be made at this last point.

Simple interpolation between the start and end date would highly underestimate gully contribution during certain years, as it could be verified when comparing average erosion rate ($39.7 \text{ ton ha}^{-1}\text{yr}^{-1}$) with punctual erosion rates at the end of the study period. Gully erosion is confirmed to be an important process of sediment generation in Mediterranean basins. Average erosion rates from gullies in the study period almost double values for similar locations and conditions obtained for rill and sheet erosion.

Further studies are needed to improve the estimations of the contribution of the different land uses to gully growth. Implementation of physically-based models of gully retreat rates and sidewall collapse could contribute to a better understanding of the processes of elongation and predict gully erosion under different scenarios, including the effect of added root cohesion to sidewall stability or gully headcut protection.



References

- Amundson, R., Berhe, A. A., Hopmans, J. W., Olson, C., Sztein, A. E. and Sparks, D. L.: Soil and human security in the 21st century, *Science*, 348(6235), doi:10.1126/science.1261071, 2015.
- 5 Campo-Bescós, M. A., Flores-Cervantes, J. H., Bras, R. L., Casalí, J. and Giráldez, J. V.: Evaluation of a gully headcut retreat model using multitemporal aerial photographs and digital elevation models, *J. Geophys. Res. Earth Surf.*, 118(4), 2012JF002668, doi:10.1002/jgrf.20147, 2013.
- Castillo, C.: Metodología de medida de la erosión por cárcavas y modelado de su control mediante diques de retención, Ph.D. diss. University of Córdoba, Dept. of Rural Engineering, <http://hdl.handle.net/10396/8521>, 2012.
- Dabney, S., Vieira, D., Yoder, D., Langendoen, E., Wells, R., and Ursic, M.: Spatially distributed sheet, rill, and ephemeral gully Erosion, *J. Hydrol. Eng., ASCE*, 20(6)C4014009, doi:10.1061/(ASCE)HE.1943-5584.0001120, 2014.
- 10 De Baets, S., Poesen, J., Reubens, B., Wemans, K., De Baerdemaeker, J. and Muys, B.: Root tensile strength and root distribution of typical Mediterranean plant species and their contribution to soil shear strength, *Pl. Soil*, 305(1-2), 207-226, doi:10.1007/s11104-008-9553-0, 2008.
- Devauchelle, O., Petroff, A. P., Seybold, H. F. and Rothman, D. H.: Ramification of stream networks, *Proc. Natnl. Acad. Sci.*, 109, 20832-20836, doi:10.1073/pnas.1215218109, 2012.
- 15 Dotterweich, M.: The history of human-induced soil erosion: Geomorphic legacies, early descriptions and research, and the development of soil conservation: A global synopsis, *Geomorphol.*, 201, 1-34, doi:10.1016/j.geomorph.2013.07.021, 2013.
- Flores-Cervantes, J. H., Istanbuluoğlu, E. and Bras, R. L.: Development of gullies on the landscape: A model of headcut retreat resulting from plunge pool erosion, *J. Geophys. Res. Earth Surf.*, 111(F1), F01010, doi:10.1029/2004JF000226, 2006.
- 20 Frankl, A., Nyssen, J., De Dapper, M., Haile, M., Deckers, J. and Poesen, J.: Trends in gully erosion as evidenced from repeat photography (North Ethiopia), *Landf. Anal.*, 17, 47-50, 2011.
- Gómez, J. A., Giráldez, J. V. and Vanwallegem, T.: Comments on “Is soil erosion in olive groves as bad as often claimed?” by L. Fleskens and L. Stroosnijder, *Geoderma*, 147(1-2), 93-95, doi:10.1016/j.geoderma.2008.07.006, 2008.
- González-Hidalgo, J. C., Peña-Monné, J. L. and de Luis, M.: A review of daily soil erosion in Western Mediterranean areas, *CATENA*, 71(2), 193-199, doi:10.1016/j.catena.2007.03.005, 2007.
- 25 Gordon, L. M., Bennett, S. J., Bingner, R. L., Theurer, F. D. and Alonso, C. V.: Simulating ephemeral gully erosion in AnnAGNPS, *Trans. ASABE*, 50(3), 857-866, 2007.
- Gordon, L. M., Bennett, S. J., Alonso, C. V. and Bingner, R. L.: Modeling long-term soil losses on agricultural fields due to ephemeral gully erosion, *J. Soil Water Conserv.*, 63(4), 173-181, doi:10.2489/jswc.63.4.173, 2008.
- 30 Kirkby, M. J. and Bracken, L. J.: Gully processes and gully dynamics, *Earth Surf. Proc. Landf.*, 34(14), 1841-1851, doi:10.1002/esp.1866, 2009.
- Martínez-Casasnovas, J. A., Ramos, M. C. and Ribes-Dasi, M.: Soil erosion caused by extreme rainfall events: mapping and quantification in agricultural plots from very detailed digital elevation models, *Geoderma*, 105(1), 125-140, 2002.



- Martínez-Casasnovas, J. A., Antón-Fernández, C. and Ramos, M. C.: Sediment production in large gullies of the Mediterranean area (NE Spain) from high-resolution digital elevation models and geographical information systems analysis, *Earth Surf. Proc. Landf.*, 28(5), 443-456, doi:10.1002/esp.451, 2003.
- Nyssen, J., Poesen, J., Veyret-Picot, M., Moeyersons, J., Haile, M., Deckers, J., Dewit, J., Naudts, J., Teka, K. and Govers, G.: Assessment of gully erosion rates through interviews and measurements: a case study from northern Ethiopia, *Earth Surf. Proc. Landf.*, 31(2), 167-185, doi:10.1002/esp.1317, 2006.
- Oostwoud Wijdenes, D. J., Poesen, J., Vandekerckhove, L. and Ghesquiere, M.: Spatial distribution of gully head activity and sediment supply along an ephemeral channel in a Mediterranean environment, *Catena*, 39(3), 147-167, 2000.
- Panagos, P., Borrelli, P., Poesen, J., Ballabio, C., Lugato, E., Meusburger, K., Montanarella, L. and Alewell, C.: The new assessment of soil loss by water erosion in Europe, *Environ. Sci. Pol.*, 54, 438-447, doi:10.1016/j.envsci.2015.08.012, 2015.
- Poesen, J., Vandekerckhove, L., Nachtergaele, J., Wijdenes, D. O., Verstraeten, G. and Van Wesemael, B.: Gully erosion in dryland environments, in Bull, L. J. and Kirkby, M. J. (Eds.) *Dryland rivers: Hydrology and Geomorphology of semi-arid channels*, John Wiley & Son, Chichester, United Kingdom, Chap. 8, 2002.
- Poesen, J., Vanwalleghem, T., de Vente, J., Knapen, A., Verstraeten, G. and Martínez-Casasnovas, J. A.: Gully erosion in Europe, in Boardman, J. and Poesen, J. (Eds.), *Soil erosion in Europe*, John Wiley & Son, Chichester, United Kingdom, Chap. 39, 2006.
- Quinton, J. N., Govers, G., Van Oost, K. and Bardgett, R. D.: The impact of agricultural soil erosion on biogeochemical cycling, *Nat. Geosci.*, 3(5), 311-314, doi:10.1038/ngeo838, 2010.
- Regnier, P., Friedlingstein, P., Ciais, P., Mackenzie, F. T., Gruber, N., Janssens, I. A., Laruelle, G. G., Lauerwald, R., Luysaert, S., Andersson, A. J., Arndt, S., Arnosti, C., Borges, A. V., Dale, A. W., Gallego-Sala, A., Godderis, Y., Goossens, N., Hartmann, J., Heinze, C., Ilyina, T., Joos, F., LaRowe, D. E., Leifeld, J., Meysman, F. J. R., Munhoven, G., Raymond, P. A., Spahni, R., Suntharalingam, P. and Thullner, M.: Anthropogenic perturbation of the carbon fluxes from land to ocean, *Nat. Geosci.*, 6(8), 597-607, 2013.
- Renard, K. G., Foster, G. R., Weesies, G. A., McCool, D. K. and Yoder, D. C.: *Predicting soil erosion by water: a guide to conservation planning with the Revised Universal Soil Loss Equation (RUSLE)*, USDA Agr. Hbk. 703, USDA, Washington, DC., 1997.
- Rengers, F. K. and Tucker, G. E.: Analysis and modeling of gully headcut dynamics, North American high plains, *J. Geophys. Res. Earth Surf.*, 119(5), 983-1003, doi:10.1002/2013JF002962, 2014.
- Saxton, N. E., Olley, J. M., Smith, S., Ward, D. P. and Rose, C. W.: Gully erosion in sub-tropical south-east Queensland, Australia, *Geomorphol.*, 173-174, 80-87, doi:10.1016/j.geomorph.2012.05.030, 2012.
- Taguas, E. V., Yuan, Y., Bingner, R. L. and Gómez, J. A.: Modeling the contribution of ephemeral gully erosion under different soil managements: A case study in an olive orchard microcatchment using the AnnAGNPS model, *CATENA*, 98, 1-16, doi:10.1016/j.catena.2012.06.002, 2012.
- Tebebu, T. Y., Abiy, A. Z., Zegeye, A. D., Dahlke, H. E., Easton, Z. M., Tilahun, S. A., Collick, A. S., Kidnau, S., Moges, S., Dadgari, F. and Steenhuis, T. S.: Surface and subsurface flow effect on permanent gully formation and upland erosion near Lake Tana in the northern highlands of Ethiopia, *Hydrol. Earth Syst. Sci.*, 14(11), 2207-2217, doi:10.5194/hess-14-2207-2010, 2010.
- Van Oost, K., Quine, T. A., Govers, G., De Gryze, S., Six, J., Harden, J. W., Ritchie, J. C., McCarty, G. W., Heckrath, G., Kosmas, C., Giráldez, J. V., da Silva, J. R. M. and Merckx, R.: The Impact of Agricultural Soil Erosion on the Global Carbon Cycle, *Science*, 318(5850), 626629, doi:10.1126/science.1145724, 2007.

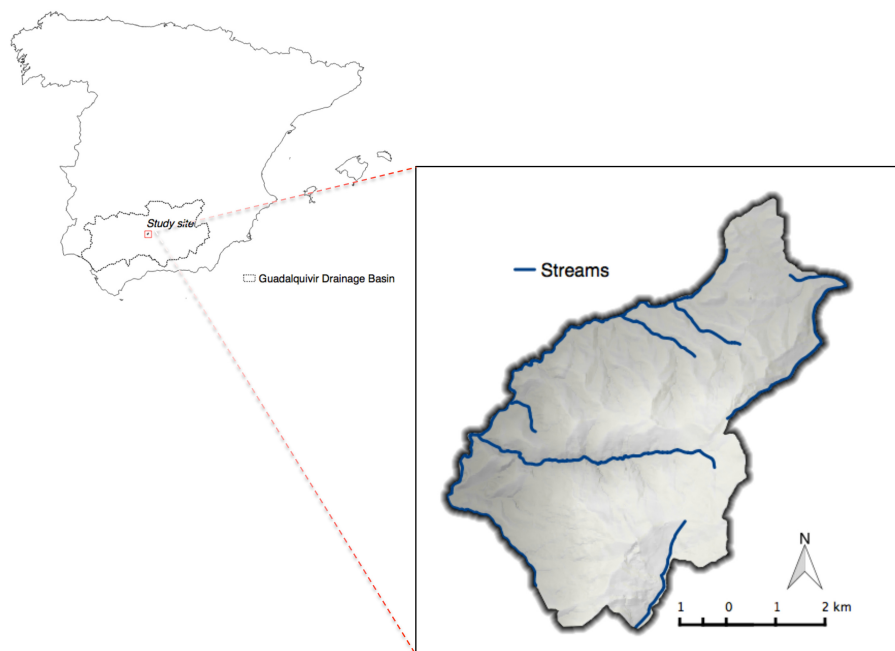


Figure 1. Site location.

Table 1. Orthophoto dataset properties.

capture year	1956	1980	1984	1999	2001	2005	2007	2009	2011	2013
resolution, m	1.0	0.5	1.0	1.0	0.5	0.5	0.5	0.5	0.5	0.5
color	b/w	b/w	b/w	b/w	b/w	col.	col.	col.	col.	col.

b/w: black and white; col.: color

Vanwalleghem, T., Bork, H. R., Poesen, J., Schmidtchen, G., Dotterweich, M., Nachtergaele, J., Bork, H., Deckers, J., Brüsch, B., Bungeneers, J. and De Bie, M.: Rapid development and infilling of a buried gully under cropland, central Belgium, *CATENA*, 63(2-3), 221243, doi:10.1016/j.catena.2005.06.005, 2005.

5 Vanwalleghem, T., Bork, H. R., Poesen, J., Dotterweich, M., Schmidtchen, G., Deckers, J., Scheers, S. and Martens, M.: Pre-historic and Roman gullying in the European oess belt: a case study from central Belgium, *The Holocene*, 16(3), 393-401, doi:10.1191/0959683606h1935rp, 2006.

Wischmeier, W. H. and Smith, D. D.: Predicting rainfall erosion losses-A guide to conservation planning., USDA Ag. Hbk. 537, USDA, Washington D.C., 1978.

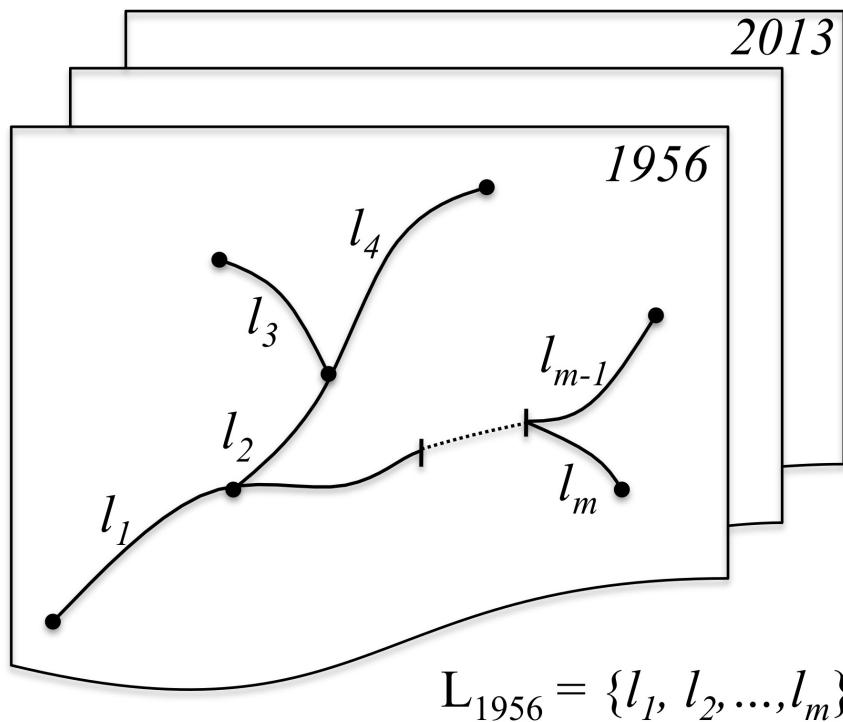


Figure 2. Illustration of the decomposition of the gully network into individual segments for the Monte Carlo-based simulation process.

Table 2. Correspondences of the simplified land use classes adopted in this study with the Map of the Land Use and Vegetation Cover of Andalusia (MUCVA, REDIAM).

MUCVA classes	Simplified classes
Herbaceous crops with scattered trees	
Non-irrigated herbaceous crops	Herbaceous crops
Irrigated herbaceous crops	
Non-irrigated tree crops: olive orchards	Olive orchards
Pasture	
Dense scrubland	Other land use
Streams and natural watercourses	
Agricultural buildings and farms	

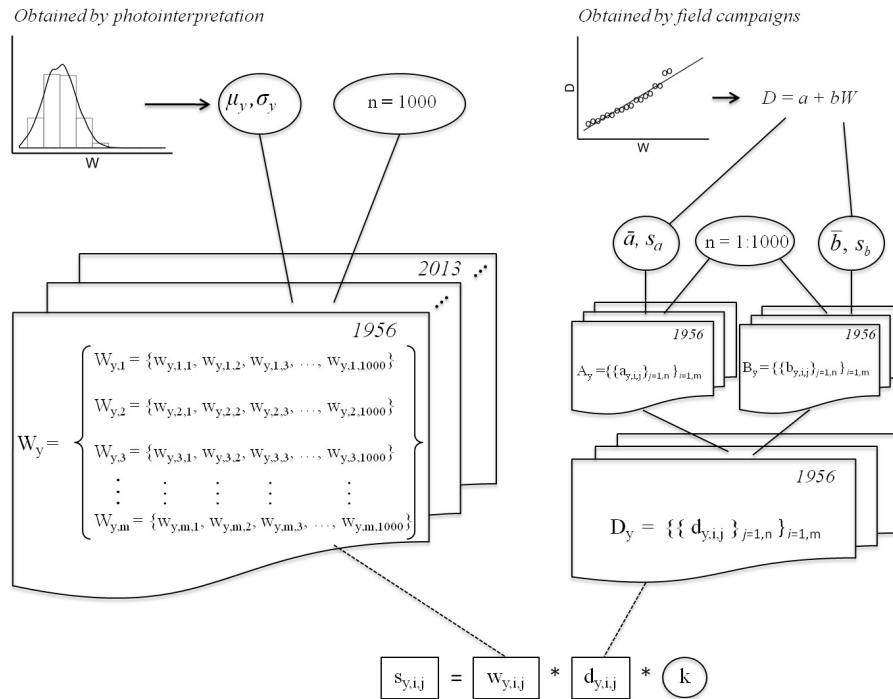


Figure 3. Conceptual scheme of the Monte Carlo simulation processes conducted to generate gully widths ($w_{y,i,j}$: single simulated width for a given segment and year, $W_{y,i}$: set of 1000 simulated widths for a given segment and year) and depths ($d_{y,i,j}$: single simulated depth for a given segment and year, $D_{y,i}$: set of 1000 simulated depths for a given segment and year) and calculate the cross section ($S_{y,i}$) for each gully segment and year. k is a shape factor for the gully cross section, m is the number of gully segment, n is the number of simulations, and a and b are fitted linear regression coefficients of the depth-width relation, with respective means (\bar{a} , \bar{b}) and standard deviations (s_a , s_b).

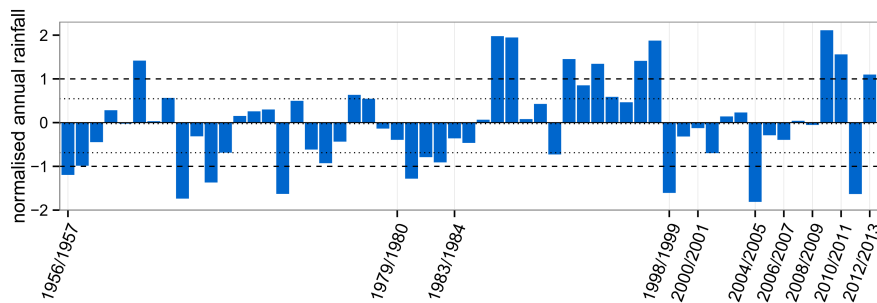


Figure 4. Standardized annual rainfall in the period 1956-2013.

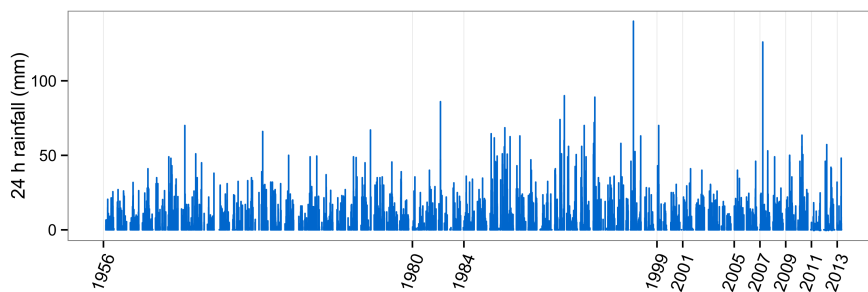


Figure 5. Daily rainfall recorded in the period 1956-2013.

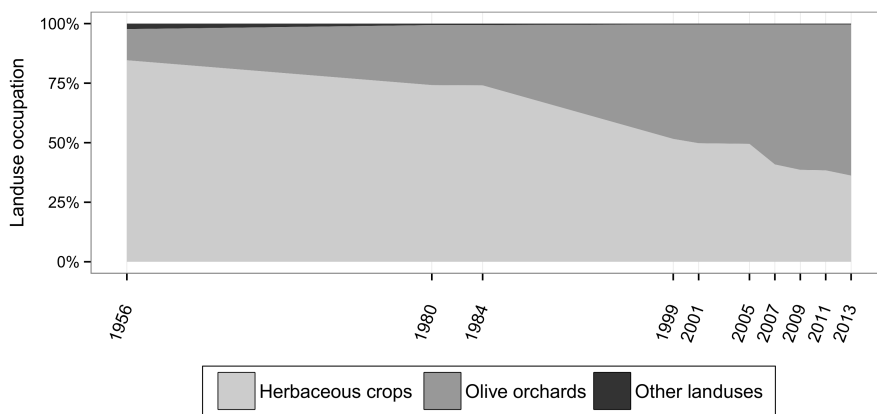


Figure 6. Land use changes in the period 1956-2013.

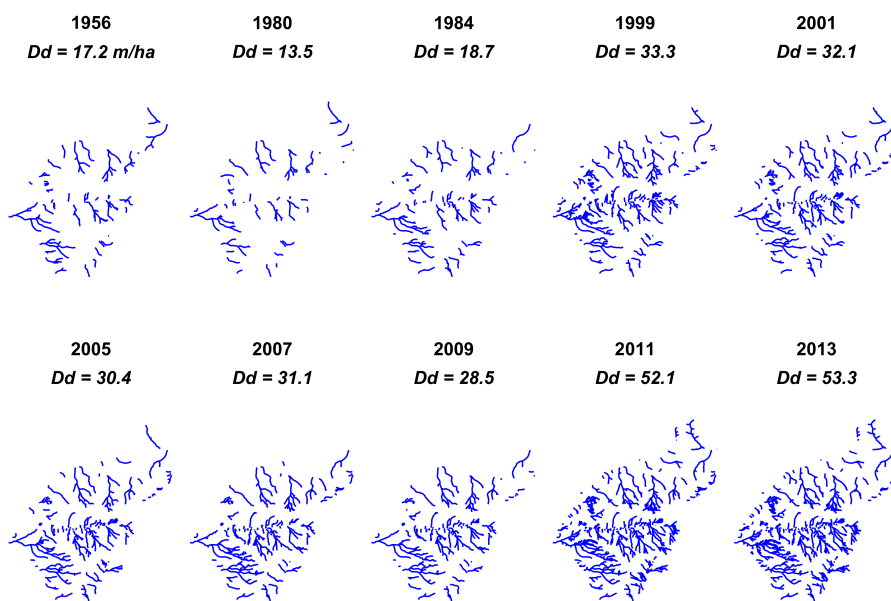


Figure 7. Gully network evolution and drainage density (D_d), in $m\ ha^{-1}$, at each period.

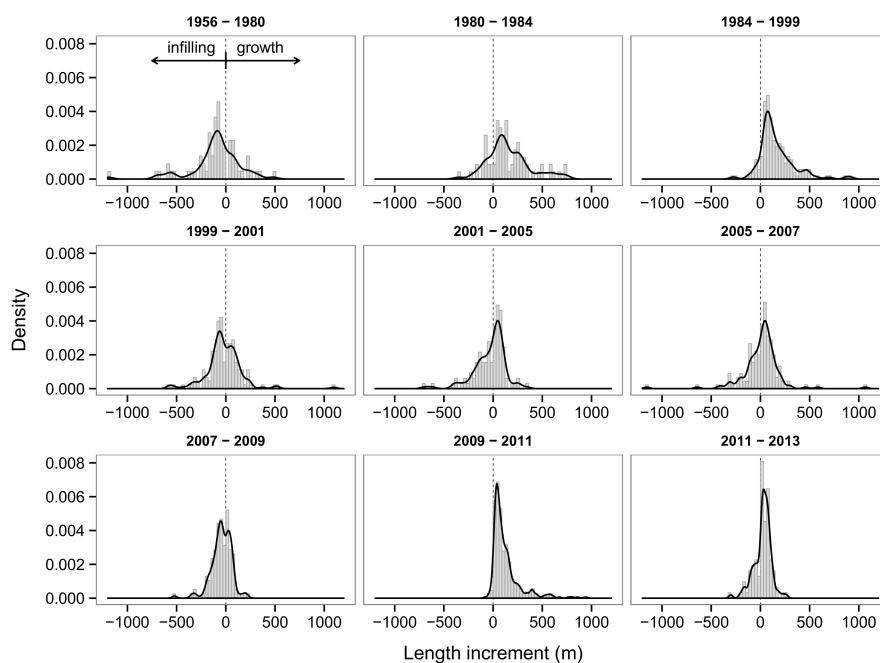


Figure 8. Gully headcut growth or decrease in the different periods between 1956 and 2013.

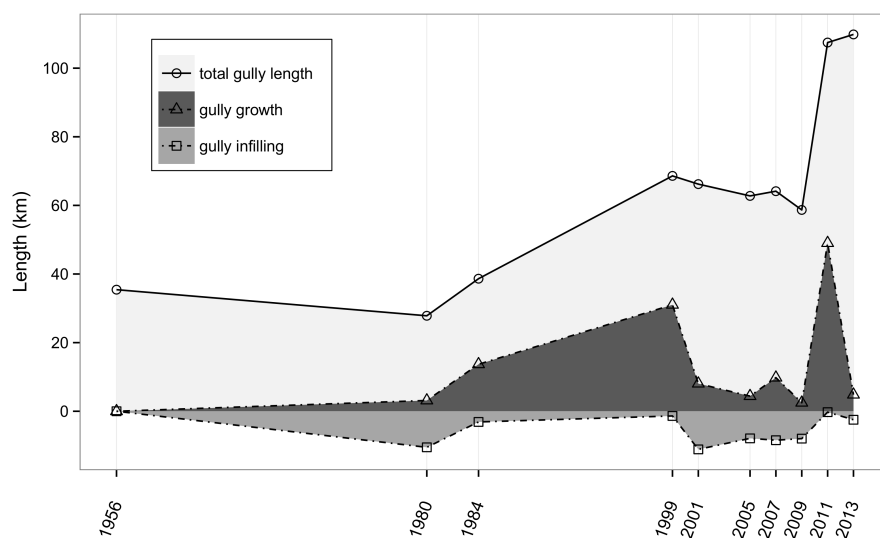


Figure 9. Gully length dynamics in the period 1956-2013.

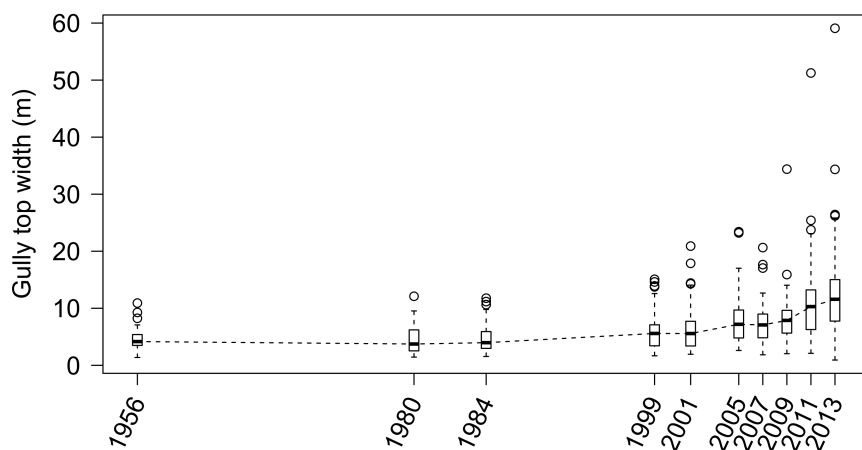


Figure 10. Gully top widths dynamics in the period 1956-2013. The dashed line indicates the mean, box and whiskers indicate the 25-50% and 5-95% quantile ranges, respectively.

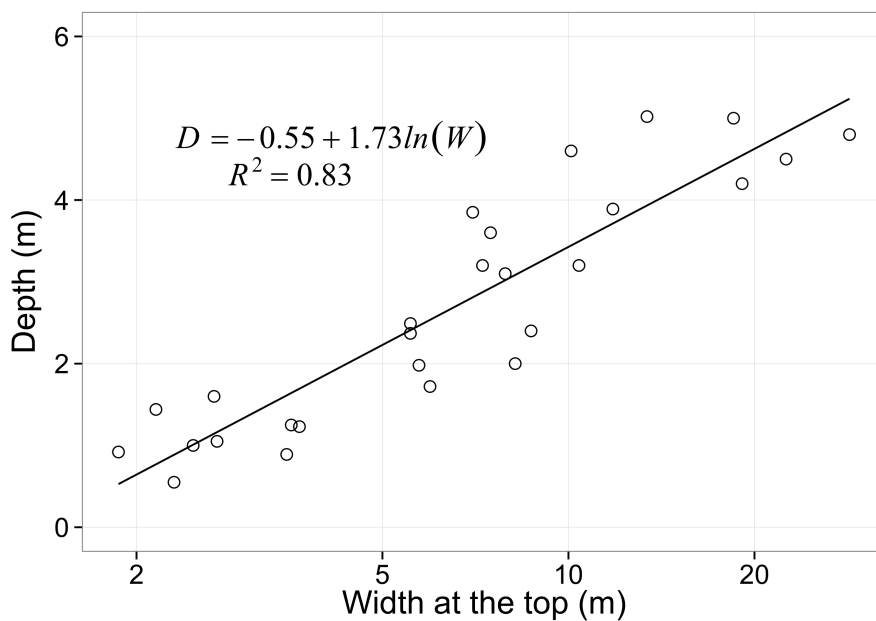


Figure 11. Width-depth relationship derived from field measurements.

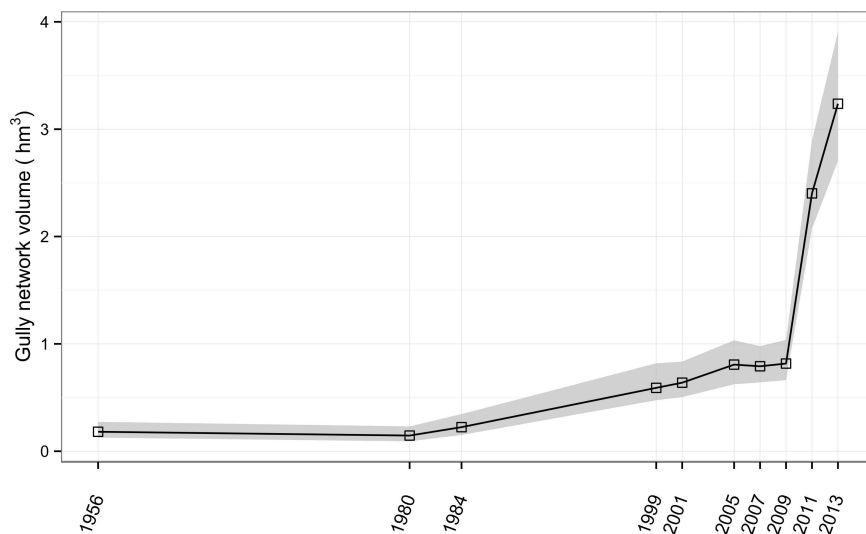


Figure 12. Gully network volume dynamics in the period 1956-2013 and uncertainty interval (grey).

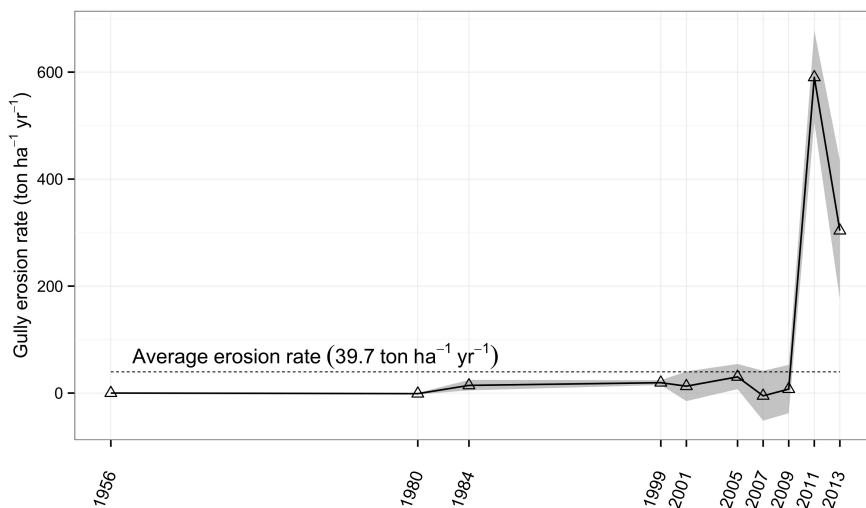


Figure 13. Gully erosion rate in $\text{ton ha}^{-1}\text{yr}^{-1}$ calculated by Monte Carlo simulation method, and average erosion rate in the period 1956-2013. The grey area represents the 90% uncertainty level



Table 3. Land use, rainfall indicators and gully growth. f_h and f_o : fractions of surface dedicated to herbaceous and olive crops, in the first year of each period. nle : number of 24 hours rainfall events per year higher than 13 mm, $nleo$: number of 24 hours rainfall events per year over the average 24 hours rainfall plus the standard deviation, R_{max} : highest daily rain depth registered within the period, MAR : Mean annual rainfall in the period. ΔL : total, and $\Delta L/\Delta t$, partial increase in gully length, and GH : gully headcut growth, averaged over the area.

period	land use			rainfall				gully growth		
	Δt <i>yr</i>	f_h	f_o	nle	$nleo$	R_{max} <i>mm</i>	MAR	ΔL <i>km</i>	$\Delta L/\Delta t$ <i>km yr⁻¹</i>	GH <i>m ha⁻¹ yr⁻¹</i>
1956		.85	.13							
1956-1980	24	.74	.25	12.9	6.8	70.0	494	-7.37	-0.31	-0.15
1980-1984	4	.74	.25	9.5	5.0	86.0	377	10.58	2.65	1.25
1984-1999	15	.52	.48	17.1	10.5	140.0	677	29.67	1.98	0.94
1999-2001	2	.50	.50	11.0	5.0	70.0	501	-3.06	-1.53	-0.72
2001-2005	4	.49	.50	11.8	4.5	41.0	438	-3.49	-0.87	-0.41
2005-2007	2	.41	.59	13.0	5.5	46.0	477	1.36	0.68	0.32
2007-2009	2	.39	.61	11.5	5.5	126.0	545	-5.48	-2.74	-1.30
2009-2011	2	.38	.61	27.5	13.0	68.5	917	48.77	24.39	11.54
2011-2013	2	.36	.63	12.5	6.0	57.2	492	2.36	1.18	0.56

Table 4. Kolmogorov-Smirnov tests (p-values) obtained by fitting observed gully widths during different years.

pdf	1956	1980	1984	1999	2001	2005	2007	2009	2011	2013
normal	0.18	0.24	0.25	0.19	0.21	0.33	0.21	0.12	0.03	0.07
gamma	0.66	0.77	0.55	0.81	0.74	0.96	0.77	0.67	0.43	0.71
lognormal	0.71	0.98	0.69	0.98	0.97	0.94	0.90	0.92	0.64	0.76
weibull	0.36	0.60	0.60	0.48	0.66	0.65	0.42	0.47	0.21	0.48

pdf: Probability distribution function